JOURNAL OF AIRCRAFT
Vol. 47, No. 4, July–August 2010

Flight Performance Analysis of Hybrid Airship: Revised Analytical Formulation

Ke-shi Zhang,* Zhong-hua Han,† and Bi-feng Song‡
Northwestern Polytechnical University, 710072 Xi'an, People's Republic of China

DOI: 10.2514/1.47294

A hybrid airship denotes one kind of aircraft that combines the use of aerodynamic and buoyant lift. It is supposed to achieve the best combination of the high-speed characteristics of the airplane and the heavy-lifting capacity of the airship. In this work, an improved flight performance analysis method for a hybrid airship is proposed, aiming to provide a set of new formulas that are more suitable for a hybrid airship. The new formulas for analyzing the steady and accelerated performances of a hybrid airship are derived in a systematic way. The main advantage of the new formulas is that the relationship between the flight performances of a hybrid airship and airplane is indicated in a clearer and simpler expression. Base on the derivation, the theoretical comparisons are performed to show the advantage and disadvantage of the hybrid airship. An example of estimating flight performance of a model hybrid airship is presented to preliminarily demonstrate and evaluate the developed method, which shows a reasonable result.

Nomenclature

C_{D0}	=	zero-lift drag coefficient
C_L	=	total lift coefficient
$C_{L\mathrm{aero}}$	=	aerodynamic lift coefficient
$C_{L\mathrm{buoy}}$	=	buoyant lift coefficient
c	=	specific fuel consumption
D	=	drag
E	=	endurance
H_C	=	airship pressure height
K	=	induced drag factor of the wing
L	=	total lift
L_{aero}	=	aerodynamic lift
L_{buoy}	=	buoyant lift
m_T	=	total mass of a hybrid airship
N_e	=	number of engines
n	=	load factor
P_A	=	power available, $\eta_{\mathrm{pr}} P_{\mathrm{es}}$
P_{es}	=	equivalent shaft power
P_R	=	power required
$P/\Delta W$	=	effective power-to-weight ratio
R	=	range
R/C	=	rate of climb
R_D	=	pull-down radius
R_P	=	pull-up radius
R_T	=	level-turn radius
S_a	=	approach distance in landing
S_{aero}	=	characteristic area of the aerodynamic lift
S_{buoy}	=	characteristic area of the buoyant lift
S_c	=	takeoff distance to clear an obstacle
S_f	=	flare distance in landing
$S_{g,\mathrm{LA}}$	=	ground roll in landing
$S_{g,\mathrm{TO}}$	=	takeoff ground roll
S_{wing}	=	wing area
T	=	thrust
U	=	flight velocity
U_{LO}	=	liftoff velocity
U_{stall}	=	stall velocity
U_V	=	sink velocity at glide flight
V_{ballonet}	=	volume of the lifting-gas ballonet inside the airship
V_{ship}	=	airship volume
W_f	=	fuel weight
W_T	=	total weight
W_1	=	weight when the fuel tank is empty
ΔW	=	$W_T - L_{\mathrm{buoy}}$, which is the designed weight supported by the aerodynamic lift
$\Delta W/S_{\mathrm{aero}}$	=	effective wing loading
η_{pr}	=	propeller efficiency
λ_A	=	the designed ratio of ΔW to total weight, $\Delta W/W_T$, $0 < \lambda_A < 1$
ρ_a	=	gas density of air
$\rho_{a,c}$	=	gas density of air at airship pressure height
ρ_h	=	gas density of lifting gas
$\rho_{h,c}$	=	gas density of lifting gas at airship pressure height
ω_D	=	pull-down rate
ω_P	=	pull-up rate
ω_T	=	level-turn rate

Subscripts

(L/D) max	=	maximum lift-to-drag ratio
(PR) min	=	minimum power required
(R/C) max	=	maximum climb rate
(RT) min	=	minimum level-turn radius
(TR) min	=	minimum thrust required
(UV) min	=	minimum sinking velocity
(θ) max	=	maximum climb angle
(ωT) max	=	maximum level-turn rate

I. Introduction

DURING the course of studies on airships, it was found that if conventional airships are used without any further modifications, their applications would be limited due to the low cruising speed and the highly inferior maneuvering properties. A hybrid airship is one kind of aircraft that combines the characteristics of heavier-than-air (HTA) (fixed-wing aircraft or helicopter) and

Presented as Paper 2009-0901 at the 47th AIAA Aerospace Sciences Meeting, Orlando, FL, 5–8 January 2009; received 21 September 2009; accepted for publication 1 February 2010.

*Associate Professor, P.O. Box 120, School of Aeronautics, No. 127 West Youyi Road; zhangkeshi@nwpu.edu.cn.

†Ph.D. Graduate, P.O. Box 754, School of Aeronautics, No. 127 West Youyi Road; hanzh@nwpu.edu.cn.

‡Professor, P.O. Box 120, School of Aeronautics, No. 127 West Youyi Road; bfsong@nwpu.edu.cn.

lighter-than-air (LTA) aircraft. In such designs, part of the weight of the aircraft and its payload are supported by the buoyant (aerostatic) lift and the remainder is supported by the aerodynamic lift. The combination of aerodynamic and buoyant lift leads to an aircraft that is a "best of both worlds" combination with the high-speed characteristics of HTA and the heavy-lifting capacity of LTA.

A variety of hybrid airship concepts had been developed by combining LTA with HTA in different ways [1] in the period from the 1960s to 1980s. These concepts include airships with wings (e.g., Megalifter), lifting-body shapes (e.g., Dynairship and Helipsoid), multiple conventional hulls (e.g., Aereon III), and combinations of buoyant hulls with rotors or rotor systems (e.g., Heli-stat, AeroCrane, and Cyclo-Crane). These studies were conducted to evaluate the feasibility, explore the new concepts, and identify the key technologies (such as the effect of buoyant ratio on flight performance, the optimal configuration of lifting-body hybrid airship, and the stability and control of the rotor hybrid airship). Although the studies had preliminarily showed that hybrid airships may be superior to conventional airships in many applications [2], no such vehicles had been produced and operated until 2000. A scale version of SkyCat at 12 m, called SkyKitten, flew in July 2000 [3]. From then on, hybrid airships received more and more interest from the industry. Hybrid Aircraft Corporation was set up and strived to introduce the best-of-breed heavy-lift cargo aircraft to the world and to revolutionize the way goods are affordably shipped. The Walrus project has been afforded by Defense Advanced Research Projects Agency to develop a heavy-lift hybrid airship. A variety of novel concepts for a hybrid airship were proposed, including a lifting-body hybrid airship (e.g., SkyCat, P-791, Aeroscraft, SkyFreigher, and Dynairship II) and a winged hybrid airship (e.g., Dynalifter), etc. The small-scale versions of P-791 successfully flew several times after 2006.

For the future development of hybrid airship technology, more fundamental research work should focus on better understanding of the mechanism of a hybrid airship and the development of a better analysis and design method. The development of a flight performance analysis method for a hybrid airship is one of the most important issues for the development of hybrid airship technology. With the flight performance analysis, the advantages and drawbacks of a hybrid airship with respect to airplane and airship can be better understood and some basic design rules and guidance can be provided to the designers. In addition, the development of a flight performance analysis method is also necessary for the development of the computer-based design of a hybrid airship. As a hybrid airship is definitely different from an airplane, the extension of the classic method for an airplane to the flight performance analysis of a hybrid airship is not exactly straightforward. The formulas for analyzing the steady and accelerated flight performances for a hybrid airship were preliminarily derived in [4], according to the classic analysis method of the aircraft performance given by Anderson [5]. The analysis method was applied to the design of new concept winged hybrid airships for different purposes, such as personal flight, planetary flight, and high-altitude flight, which provided a very good reference to other researchers in the same community. However, in the present authors' points of view, the analysis method presented in [4] needs to be further improved, both for better prediction of the flight performance of a hybrid airship and for better understanding of the characteristics of a hybrid airship.

This paper is motivated by further improvement of the flight performance analysis method of a hybrid airship. The goal of this paper is to systematically derive new formulas for the analysis and prediction of the flight performances of a hybrid airship. The formulas for analyzing the steady and accelerated flight performances of a hybrid airship are derived to be the simplest expressions. As the hybrid airships are generally propeller-driven, these formulas are derived by taking the propeller-driven airplane as reference. Special attention is paid to address the requirements of indicating the relationship between the flight performances of a hybrid airship and airplane and identifying the advantage of the hybrid airship. An example of analyzing the flight performance of a modeled hybrid airship is presented to preliminarily demonstrate and evaluate the developed method in this paper.

II. Lift and Drag Coefficients of Hybrid Airship

For a hybrid airship, the buoyant lift is created by lifting gas in the airship and the aerodynamic lift is created by the lifting surface. The lift and drag coefficients of a hybrid airship will be defined in this section.

A. Lift Coefficient

As the buoyancy lift is affected by ρ_a, ρ_h, and V_{ship}, the buoyant lift coefficient is defined as

$$C_{L\text{buoy}} = \frac{L_{\text{buoy}}}{\rho_a g V_{\text{ship}}} \tag{1}$$

where the buoyant lift can be calculated by

$$L_{\text{buoy}} = (\rho_a - \rho_h) g V_{\text{ballonet}} \tag{2}$$

when flying under airship pressure height (i.e., $H \le H_C$). (The airship pressure height [6] is defined as the height at which the ballonets are fully deflated and is therefore the maximum height to which the airship can climb without overpressuring the envelope or venting gas.) According to the principle of mass conservation,

$$\rho_{h,c} \cdot V_{\text{ship}} = \rho_h \cdot V_{\text{ballonet}} \tag{3}$$

Substituting Eqs. (2) and (3) into Eq. (1), we have

$$C_{L\text{buoy}} = \left(1 - \frac{\rho_h}{\rho_a}\right) \cdot \frac{\rho_{h,c}}{\rho_h} \tag{4}$$

The aerodynamic lift coefficient is defined as same as that for airplane. It is written as

$$C_{L\text{aero}} = \frac{L_{\text{aero}}}{\frac{1}{2}\rho_a U^2 S_{\text{aero}}} \tag{5}$$

It is noted that S_{aero} is the reference area of lifting surface. It should be specially defined according to different geometries of the hybrid airships. In the case of winged hybrid airship with conventional revolution airship body, S_{aero} is equal to S_{wing}. In the case of lifting-body hybrid airship, it corresponds to the reference area of the airship body.

The total lift coefficients of a hybrid airship are defined in Eq. (6):

$$C_L = \frac{L}{\frac{1}{2}\rho_a U^2 S_{\text{aero}}} = C_{L\text{buoy}} R_F + C_{L\text{aero}} \tag{6}$$

where

$$R_F = \frac{g V_{\text{ship}}}{\frac{1}{2} U^2 S_{\text{aero}}} \tag{7}$$

It is noted that although $C_{L\text{buoy}}$ is independent of velocity, R_F is actually the function of velocity.

B. Drag Coefficient

The drag coefficient is defined as

$$C_D = \frac{D}{\frac{1}{2}\rho_a U^2 S_{\text{aero}}} \tag{8}$$

As the aerodynamic lift is totally generated by the lifting surface, the total drag coefficient can also be written as

$$C_D = C_{D0} + K C_{L\text{aero}}^2 \tag{9}$$

III. Analysis of Steady Flight Performance

The following analysis of the steady flight performance and the accelerated flight performance for a hybrid airship is similar to the classic analysis of airplane flight performance given by Anderson [5]. If $\lambda_A = 1$, the hybrid airship is actually an airplane.

In this section the new formulas for analyzing the thrust required, the maximum lift-to-drag ratio, the minimum power required, the stalling velocity, the rate of climb, the range, and the endurance for steady flight are derived.

A. Thrust Required for Steady, Level Flight

Assuming the thrust aligned with the flight direction, the thrust required for level flight overcomes the drag at a given speed and altitude. It is given by

$$T_R = D = \tfrac{1}{2}\rho_a U^2 S_{\text{aero}}(C_{D0} + KC_{L\text{aero}}^2) \tag{10}$$

Because of steady level flight,

$$C_{L\text{aero}} = \frac{L_{\text{aero}}}{\frac{1}{2}\rho_a U^2 S_{\text{aero}}} = \frac{\Delta W}{\frac{1}{2}\rho_a U^2 S_{\text{aero}}} \tag{11}$$

Substituting Eq. (11) into Eq. (10) and rearranging, we obtain

$$\frac{1}{2}\rho_a^2 U^4 S_{\text{aero}} C_{D0} - T_R \rho_a U^2 + 2KS_{\text{aero}}\left(\frac{\Delta W}{S_{\text{aero}}}\right)^2 = 0 \tag{12}$$

Taking the square root of Eq. (12), the final expression for velocity is obtained

$$U = \left(\frac{(T_R/\Delta W)(\Delta W/S_{\text{aero}}) \pm (\Delta W/S_{\text{aero}})\sqrt{(T_R/\Delta W)^2 - 4KC_{D0}}}{\rho_a C_{D0}}\right)^{1/2} \tag{13}$$

When the discriminant in Eq. (13) equals zero, only one velocity is obtained and its corresponding thrust is the minimum thrust required for steady level flight (as expressed below):

$$U_{(TR)\min} = \left(\frac{2}{\rho_a}\sqrt{\frac{K}{C_{D0}}}\frac{\Delta W}{S_{\text{aero}}}\right)^{1/2} \tag{14}$$

$$T_{(R)\min} = \lambda_A \cdot W_T\sqrt{4KC_{D0}} \quad \text{or} \quad (T_R/\Delta W)_{\min} = \sqrt{4KC_{D0}} \tag{15}$$

B. Maximum Lift-to-Drag Ratio

The lift-to-drag ratio of a hybrid airship is generally calculated by

$$\frac{L}{D} = \frac{C_L}{C_D} = \frac{C_L}{C_{D0} + KC_{L\text{aero}}^2} \tag{16}$$

Rearranging Eq. (6) to $C_{L\text{aero}} = C_L - R_F C_{L\text{buoy}}$ and substituting it into Eq. (16), we get

$$\frac{L}{D} = \frac{C_L}{C_D} = \frac{C_L}{C_{D0} + K(C_L - R_F C_{L\text{buoy}})^2} \tag{17}$$

For maximizing L/D, differentiate Eq. (17) with respect to C_L and set the result equal to zero. Note that R_F is also the function of C_L. So the expression of R_F with respect to C_L should be derived before differentiating Eq. (17). Because of steady level flight,

$$W_T = L = C_L \cdot \tfrac{1}{2}\rho_a U^2 S_{\text{aero}} \tag{18}$$

Rearranging Eq. (18) and substituting it into Eq. (7), the expression for R_F with respect to C_L is obtained as

$$R_F = \frac{\rho_a g V_{\text{ship}}}{W_T} \cdot C_L \tag{19}$$

Substituting Eq. (19) into Eq. (17), we obtain

$$\frac{L}{D} = \frac{C_L}{C_{D0} + K(1 - \frac{\rho_a g V_{\text{ship}}}{W_T} C_{L\text{buoy}})^2 C_L^2} \tag{20}$$

Because $L_{\text{buoy}} = C_{L\text{buoy}} \cdot \rho_a g V_{\text{ship}}$ and $\lambda_A = (1 - L_{\text{buoy}}/W_T)$, Eq. (20) can be simplified into the final expression:

$$\frac{L}{D} = \frac{C_L}{C_{D0} + K\lambda_A^2 C_L^2} \tag{21}$$

Since Eqs. (11) and (18) and $\Delta W = \lambda_A W_T$ hold for steady level flight, there must be

$$C_{L\text{aero}} = \lambda_A C_L \tag{22}$$

Note that the derivation for Eq. (21) can be simplified by substituting Eq. (22) directly into Eq. (16). But the above derivation is more useful for the comparison with that in [4].

Differentiating Eq. (21) with respect to C_L and setting the result equal to zero, the lift coefficient at maximum L/D is obtained as

$$C_{L,(L/D)\max} = \frac{1}{\lambda_A}\sqrt{\frac{C_{D0}}{K}} \tag{23}$$

The aerodynamic lift coefficient at maximum L/D can be derived by substituting Eq. (23) into Eq. (22), which is

$$C_{L\text{aero},(L/D)\max} = \sqrt{\frac{C_{D0}}{K}} \tag{24}$$

Substitute Eq. (23) into Eq. (21) and the final expression of $(L/D)_{\max}$ can be written as

$$\left(\frac{L}{D}\right)_{\max} = \frac{1}{\lambda_A}\sqrt{\frac{1}{4KC_{D0}}} \tag{25}$$

Since $L = W_T$ for steady level flight,

$$U = \sqrt{\frac{2W_T}{\rho_a S_{\text{aero}} \cdot C_L}} \tag{26}$$

Substituting Eq. (23) into Eq. (26), the expression of velocity at which $(L/D)_{\max}$ is achieved is

$$U_{(L/D)\max} = \sqrt{\frac{2}{\rho_a} \cdot \sqrt{\frac{K}{C_{D0}}} \cdot \frac{\Delta W}{S_{\text{aero}}}} \tag{27}$$

Comparing Eq. (27) with Eq. (14) it can be concluded that minimum T_R occurs when L/D is maximum, as with an airplane.

C. Minimum Power Required for Steady Level Flight

The power required is generally written as

$$P_R = T_R \cdot U = D \cdot U = \frac{L}{L/D} \cdot U \tag{28}$$

Since Eq. (18) holds for steady level flight, we obtain

$$P_R = \frac{W_T}{C_L/C_D} \cdot \sqrt{\frac{2W_T}{\rho_a S_{\text{aero}} \cdot C_L}} \tag{29}$$

or the simplified expression

$$P_R = \sqrt{\frac{2W_T^3 C_D^2}{\rho_a S_{\text{aero}} \cdot C_L^3}} \quad \text{or} \quad P_R = \sqrt{\frac{2\Delta W^3 C_D^2}{\rho_a S_{\text{aero}} C_{L\text{aero}}^3}} \tag{30}$$

As $P_R \propto (C_L^{3/2}/C_D)^{-1}$, the minimum power required occurs when $(C_L^{3/2}/C_D)_{\max}$ is achieved.

$C_L^{3/2}/C_D$ can be written as

$$\frac{C_L^{3/2}}{C_D} = \frac{C_L^{3/2}}{C_{D0} + KC_{L\text{aero}}^2} \tag{31}$$

Rearranging Eq. (6) to $C_{L\text{aero}} = C_L - R_F C_{L\text{buoy}}$ and substituting it into Eq. (31), we get

$$C_L^{3/2}/C_D = \frac{C_L^{3/2}}{C_{D0} + K(C_L - R_F C_{L\text{buoy}})^2} \tag{32}$$

Substituting Eq. (19) and Eq. (1) into Eq. (32), the following equation is obtained:

$$C_L^{3/2}/C_D = \frac{C_L^{3/2}}{C_{D0} + K\lambda_A^2 C_L^2} \tag{33}$$

Note that the derivation for Eq. (33) can be simplified by substituting Eq. (22) directly into Eq. (31). But the above derivation is more useful for the comparison with that in [4]. To maximize $C_L^{3/2}/C_D$, differentiate Eq. (33) with respect to C_L and set the result equal to zero; we then have

$$C_{L,(C_L^{3/2}/C_D)\max} = \frac{1}{\lambda_A}\sqrt{\frac{3C_{D0}}{K}} \tag{34}$$

Substituting Eq. (34) into Eq. (33), we have

$$(C_L^{3/2}/C_D)_{\max} = \frac{1}{\lambda_A^{3/2}} \cdot \frac{1}{4}\left(\frac{3}{KC_{D0}^{1/3}}\right)^{3/4} \tag{35}$$

So the minimum power required for steady level flight is

$$P_{(R)\min} = \sqrt{\frac{32\Delta W^2}{\rho_a} \cdot \frac{\Delta W}{S_{\text{aero}}} \cdot \left(\frac{KC_{D0}^{1/3}}{3}\right)^{3/2}} \tag{36}$$

Since Eq. (26) holds for steady level flight, the velocity at which P_R is minimum occurs at

$$U_{(PR)\min} = U_{(C_L^{3/2}/C_D)\max} = \left(\frac{2}{\rho_a} \cdot \frac{\Delta W}{S_{\text{aero}}}\sqrt{\frac{K}{3C_{D0}}}\right)^{1/2} \tag{37}$$

D. Maximum Velocity and Stalling Velocity

For the propeller-driven hybrid airship, the power available is essentially constant with velocity. The high-speed intersection of the maximum-power-available curve and the power-required curve defines the maximum velocity for straight and level flight. The low-speed intersection seems to define the minimum velocity. However, it is more likely that the stall velocity is encountered before reaching the minimum velocity.

When $C_L = C_{L\max}$ the corresponding value of velocity is the stalling velocity, which is expressed as

$$U_{\text{stall}} = \sqrt{\frac{2}{\rho_a} \cdot \frac{W_T}{S_{\text{aero}}} \cdot \frac{1}{C_{L\max}}} \tag{38}$$

Since Eq. (22) holds for steady level flight, C_L achieves maximum when $(C_{L,\text{aero}})_{\max}$ is achieved. Substituting $\Delta W = \lambda_A W_T$ and Eq. (22) into Eq. (38), the stalling velocity can also be written as

$$U_{\text{stall}} = \sqrt{\frac{2}{\rho_a} \cdot \frac{\Delta W}{S_{\text{aero}}} \cdot \frac{1}{C_{(L\text{aero})\max}}} \tag{39}$$

It is shown that the stalling velocity of the hybrid airship only depends on the flight altitude, the effective wing loading, and the maximum lift coefficient of the wing.

E. Rate of Climb

Assuming the thrust line is in the direction of flight, the force and velocity for climbing flight of a hybrid airship are shown in Fig. 1. The accelerated climb is out of the scope of this study.

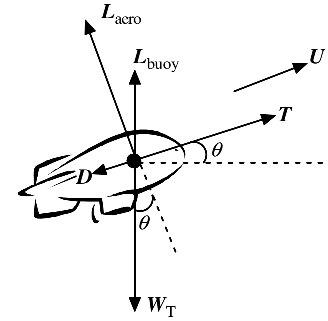

Fig. 1 Force and velocity diagram for climbing flight.

As shown in Fig. 1, the equations of motion for a climbing hybrid airship can be written as

$$T + L_{\text{buoy}}\sin\theta - D - W_T\sin\theta = 0 \tag{40}$$

$$L_{\text{aero}} + L_{\text{buoy}}\cos\theta - W_T\cos\theta = 0 \tag{41}$$

Multiplying Eq. (40) by $U/\Delta W$ and rearranging it, we have

$$U\sin\theta = R/C = \frac{TU - DU}{\Delta W} \tag{42}$$

From Eq. (5) and Eq. (41),

$$C_{L\text{aero}} = \frac{\Delta W\cos\theta}{\frac{1}{2}\rho_a U^2 S_{\text{aero}}} \tag{43}$$

Since

$$D = \tfrac{1}{2}\rho_a U^2 S_{\text{aero}} \cdot C_D = \tfrac{1}{2}\rho_a U^2 S_{\text{aero}} \cdot (C_{D0} + KC_{L\text{aero}}^2) \tag{44}$$

Substituting Eq. (43) into Eq. (44), one can obtain the formula below after simplification:

$$D = \frac{1}{2}\rho_a U^2 S_{\text{aero}} \cdot C_{D0} + \frac{K\Delta W^2(\cos\theta)^2}{\frac{1}{2}\rho_a U^2 S_{\text{aero}}} \tag{45}$$

Substituting Eq. (45) into Eq. (42), the final expression of R/C can be written as

$$R/C = U\sin\theta = U\left(\frac{T}{\Delta W} - \frac{1}{2}\rho_a U^2 C_{D0}\left(\frac{\Delta W}{S_{\text{aero}}}\right)^{-1} - \frac{\Delta W}{S_{\text{aero}}} \cdot \frac{K(\cos\theta)^2}{\frac{1}{2}\rho_a U^2}\right) \tag{46}$$

In [5] the assumption of $\cos\theta \approx 1$ is made for the climb performance analysis of airplanes, because the climb angles of conventional airplanes are usually less than 15 deg. However, the climb angle of a hybrid airship largely depends on λ_A. If λ_A is closer to 1, ΔW approaches W_T and the climb performance of a hybrid airship is similar to that of an airplane. In contrast, if λ_A is closer to 0, the climb angle must be similar to that of an airship and much larger than that of an airplane. If λ_A is equal to zero, the climb angle must be 90 deg. In this case, the assumption of $\cos\theta \approx 1$ is not reasonable. In the paragraphs below, the climb performance of a hybrid airship will be discussed with and without the assumption of $\cos\theta \approx 1$, respectively.

Assuming $\cos\theta = 1$: This assumption is made when the climb angle is less than 15 deg. From Eq. (46),

$$U\sin\theta = U\left(\frac{T}{\Delta W} - \frac{1}{2}\rho_a U^2 C_{D0}\left(\frac{\Delta W}{S_{\text{aero}}}\right)^{-1} - \frac{\Delta W}{S_{\text{aero}}} \cdot \frac{K}{\frac{1}{2}\rho_a U^2}\right) \tag{47}$$

$$\sin\theta = \frac{T}{\Delta W} - \frac{1}{2}\rho_a U^2 C_{D0}\left(\frac{\Delta W}{S_{\text{aero}}}\right)^{-1} - \frac{\Delta W}{S_{\text{aero}}} \cdot \frac{K}{\frac{1}{2}\rho_a U^2} \tag{48}$$

Since a hybrid airship is generally propeller-driven, the available thrust can be written as

$$T_A = \frac{\eta_{\mathrm{pr}} P_{\mathrm{es}}}{U} \tag{49}$$

Substituting Eq. (49) into Eq. (48),

$$\sin\theta = \frac{\eta_{\mathrm{pr}} P_{\mathrm{es}}}{U \Delta W} - \frac{1}{2}\rho_a U^2 C_{D0}\left(\frac{\Delta W}{S_{\mathrm{aero}}}\right)^{-1} - \frac{\Delta W}{S_{\mathrm{aero}}} \cdot \frac{K}{\frac{1}{2}\rho_a U^2} \tag{50}$$

For maximizing the climb angle, differentiate Eq. (50) with respect to U and set the result equal to zero. We have

$$U^4 + \frac{\eta_{\mathrm{pr}}(P_{\mathrm{es}}/\Delta W)(\Delta W/S_{\mathrm{aero}})}{\rho_a C_{D0}} U - \frac{4(\Delta W/S_{\mathrm{aero}})^2 K}{\rho_a^2 C_{D0}} = 0 \tag{51}$$

For a propeller-driven aircraft, the magnitudes of the last two terms in Eq. (51) are much larger than that of the first term [7], and the velocity for the maximum climbing angle can be approximated as

$$U_{(\theta)\max} \approx \frac{4(\Delta W/S_{\mathrm{aero}})K}{\rho_a \eta_{\mathrm{pr}}(P_{\mathrm{es}}/\Delta W)} \tag{52}$$

Substituting Eq. (52) into Eq. (50), the final expression of $\theta_{\max}$ can be obtained:

$$\theta_{\max} = \arcsin\left(\frac{\rho_a \eta_{\mathrm{pr}}^2 (P_{\mathrm{es}}/\Delta W)^2}{8K(\Delta W/S_{\mathrm{aero}})} - \frac{8K^2 C_{D0}(\Delta W/S_{\mathrm{aero}})}{\rho_a \eta_{\mathrm{pr}}^2 (P_{\mathrm{es}}/\Delta W)^2}\right) \tag{53}$$

or

$$\theta_{\max} = \arcsin\left(f - \frac{KC_{D0}}{f}\right), \qquad f = \frac{\rho_a \eta_{\mathrm{pr}}^2 (P_{\mathrm{es}}/\Delta W)^2}{8K(\Delta W/S_{\mathrm{aero}})} \tag{54}$$

For a propeller-driven aircraft, maximum climb rate occurs at the flight velocity for minimum power required [5]. The flight velocity for maximum climb rate is

$$U_{(R/C)\max} = U_{(PR)\min} = \left(\frac{2}{\rho_a}\sqrt{\frac{K}{3C_{D0}}} \cdot \frac{\Delta W}{S_{\mathrm{aero}}}\right)^{1/2} \tag{55}$$

Since $(L/D)_{\max}$ in Eq. (25), by substituting Eqs. (49) and (55) into Eq. (47), one can obtain the maximum climb rate after simplifications:

$$(R/C)_{\max} = \frac{1}{\lambda_A}\left(\frac{\eta_{\mathrm{pr}} P_{\mathrm{es}}}{W_T} - \left(\frac{2}{\rho_a}\sqrt{\frac{K}{3C_{D0}}} \cdot \frac{\Delta W}{S_{\mathrm{aero}}}\right)^{1/2} \cdot \frac{1.155}{(L/D)_{\max}}\right) \tag{56}$$

Since $\sin\theta = (R/C)/U$,

$$\theta_{(R/C)\max} = \arcsin\left(\frac{1}{\lambda_A}\frac{\eta_{\mathrm{pr}} P_{\mathrm{es}}}{W_T} - \left(\frac{2}{\rho_a}\sqrt{\frac{K}{3C_{D0}}} \cdot \frac{\Delta W}{S_{\mathrm{aero}}}\right)^{1/2} \cdot 1.155\sqrt{4KC_{D0}}\right) \tag{57}$$

Assuming $\cos\theta \neq 1$: In the following paragraphs, a more general way will be applied for the derivation of maximum climb rate. The flight velocity for maximum climb rate is the same as that in Eq. (55). Substituting Eq. (49) into Eq. (46), the following expression is obtained:

$$R/C = \frac{\eta_{\mathrm{pr}} P_{\mathrm{es}}}{\Delta W} - U\left(\frac{1}{2}\rho_a U^2 C_{D0}\left(\frac{\Delta W}{S_{\mathrm{aero}}}\right)^{-1} + \frac{\Delta W}{S_{\mathrm{aero}}} \cdot \frac{K}{\frac{1}{2}\rho_a U^2} \cdot (1 - (\sin\theta)^2)\right) \tag{58}$$

Substituting $\sin\theta = (R/C)/U$ into Eq. (58), we have

$$R/C = \frac{\eta_{\mathrm{pr}} P_{\mathrm{es}}}{\Delta W} - U\left(\frac{1}{2}\rho_a U^2 C_{D0}\left(\frac{\Delta W}{S_{\mathrm{aero}}}\right)^{-1} + \frac{\Delta W}{S_{\mathrm{aero}}} \cdot \frac{K}{\frac{1}{2}\rho_a U^2} \cdot \left(1 - \left(\frac{R/C}{U}\right)^2\right)\right) \tag{59}$$

Since Eq. (55) holds, the dynamic pressure at which R/C achieves maximum is

$$q_{(R/C)\max} = \frac{1}{2}\rho_a U_{(R/C)\max}^2 = \sqrt{\frac{K}{3C_{D0}}} \cdot \frac{\Delta W}{S_{\mathrm{aero}}} \tag{60}$$

Substituting Eq. (60) into Eq. (59) and defining $A = \sqrt{KC_{D0}}$ and $B = \eta_{\mathrm{pr}} P_{\mathrm{es}}/\Delta W$, the following expression is obtained:

$$(R/C)_{\max}^2 - \frac{1}{\sqrt{3}}\frac{U_{(R/C)\max}}{A}(R/C)_{\max} + \frac{1}{\sqrt{3}}\frac{U_{(R/C)\max}}{A}B - \frac{4}{3}U_{(R/C)\max}^2 = 0 \tag{61}$$

Taking the square root of Eq. (61),

$$(R/C)_{\max} = \frac{1}{2\sqrt{3}}\left(\frac{U_{(R/C)\max}}{A} \pm \sqrt{\left(\frac{U_{(R/C)\max}}{A}\right)^2 - 4\sqrt{3}B \cdot \frac{U_{(R/C)\max}}{A} + 16U_{(R/C)\max}^2}\right) \tag{62}$$

According to our studies, the expression below is reasonable for maximum climb rate:

$$(R/C)_{\max} = \frac{1}{2\sqrt{3}}\left(\frac{U_{(R/C)\max}}{A} - \sqrt{\left(\frac{U_{(R/C)\max}}{A}\right)^2 - 4\sqrt{3}B \cdot \frac{U_{(R/C)\max}}{A} + 16U_{(R/C)\max}^2}\right) \tag{63}$$

The climb angle at which R/C achieves maximum is

$$\theta_{(R/C)\max} = \arcsin\left(\frac{(R/C)_{\max}}{U_{(R/C)\max}}\right) \tag{64}$$

F. Glide Flight

For steady unaccelerated descent of a hybrid airship, where θ is the equilibrium glide angle, the forces are shown in Fig. 2 and the equations of motion are written as Eq. (65):

$$L_{\mathrm{aero}} = W_T\cos\theta - L_{\mathrm{buoy}}\cos\theta = \Delta W\cos\theta \tag{65}$$

$$D = W_T\sin\theta - L_{\mathrm{buoy}}\sin\theta = \Delta W\sin\theta \tag{66}$$

Dividing Eq. (66) by Eq. (65), we obtain

$$\tan\theta = \frac{1}{L_{\mathrm{aero}}/D} = \frac{1}{C_{L\mathrm{aero}}/C_D} \tag{67}$$

From Eq. (65), it can be concluded that

$$U = \sqrt{\frac{2\cos\theta}{\rho_a C_{L\mathrm{aero}}} \cdot \frac{\Delta W}{S_{\mathrm{aero}}}} \tag{68}$$

Multiplying Eq. (68) by $\sin\theta$, the rate of descent following can be obtained:

$$U_V = U\sin\theta = \sin\theta\sqrt{\frac{2\cos\theta}{\rho_a C_{L\mathrm{aero}}} \cdot \frac{\Delta W}{S_{\mathrm{aero}}}} \tag{69}$$

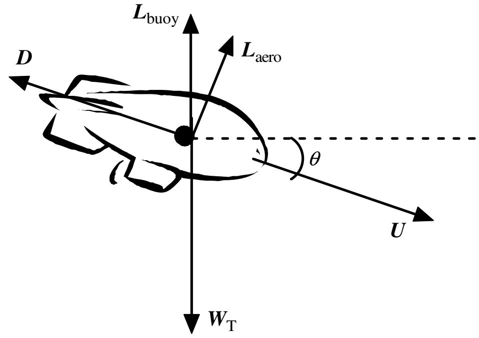

Fig. 2 Force and velocity diagram for gliding flight.

Reorganizing Eq. (67) and substituting it into Eq. (69), we get

$$U_V = \sqrt{\frac{2\cos^3\theta}{\rho_a C_{L\text{aero}}^3/C_D^2} \cdot \frac{\Delta W}{S_{\text{aero}}}} \tag{70}$$

The lift-to-drag ratio largely depends on λ_A, as shown in Eq. (25). The design of a hybrid airship must make a compromise between aerodynamic lift and buoyant lift to obtain higher L/D instead of higher L_{aero}/D. So L_{aero}/D of the hybrid airship is not essentially higher than that of the airplane. When θ is no more than 15°, i.e., L_{aero}/D is no less than 3.73 according to Eq. (67), it is reasonable to make the assumption of $\cos\theta \approx 1$. Then Eq. (70) can be rewritten as

$$U_V = \sqrt{\frac{2}{\rho_a C_{L\text{aero}}^3/C_D^2} \cdot \frac{\Delta W}{S_{\text{aero}}}} \tag{71}$$

As $U_V \propto (C_{L\text{aero}}^{3/2}/C_D)^{-1}$, the minimum sinking velocity occurs when $(C_{L\text{aero}}^{3/2}/C_D)_{\max}$ is achieved. Differentiate the following expression of $C_{L\text{aero}}^{3/2}/C_D$ with respect to $C_{L\text{aero}}$,:

$$C_{L\text{aero}}^{3/2}/C_D = \frac{C_{L\text{aero}}^{3/2}}{C_{D0} + kC_{L\text{aero}}^2} \tag{72}$$

and set it equal to zero. We have

$$C_{L\text{aero},(C_{L\text{aero}}^{3/2}/C_D)\max} = \sqrt{\frac{3C_{D0}}{k}} \tag{73}$$

Substituting Eq. (73) into Eq. (71), the minimum sinking velocity can be derived as

$$U_{(V)\min} = \sqrt{\frac{32}{\rho_a} \cdot \frac{\Delta W}{S_{\text{aero}}} \cdot \left(\frac{kC_{D0}^{1/3}}{3}\right)^{3/2}} \tag{74}$$

G. Range and Endurance

The classical Breguet range equation is applicable for a propeller-driven hybrid airship, as shown in Eq. (75):

$$R = \frac{\eta_{\text{pr}}}{c} \cdot \frac{L}{D} \ln \frac{W_T}{W_1} \tag{75}$$

The detailed derivation of this equation can be found in [5].

For maximum range, the hybrid airship should fly at maximum L/D in addition to improving propeller efficiency, reducing specific fuel consumption, and carrying more fuel. Since $(L/D)_{\max}$ in Eq. (25), the maximum range is derived as

$$R_{\max} = \frac{1}{\lambda_A} \cdot \frac{\eta_{\text{pr}}}{c} \sqrt{\frac{1}{4KC_{D0}}} \ln \frac{W_T}{W_1} \tag{76}$$

The endurance for a propeller-driven aircraft can be written as [5]

$$E = \frac{\eta_{\text{pr}}}{c} \sqrt{2\rho_a S_{\text{aero}}} \frac{C_L^{3/2}}{C_D} (W_1^{-1/2} - W_T^{-1/2}) \tag{77}$$

From Eq. (77) it can be concluded that for maximum endurance, a hybrid airship should flying at maximum $C_L^{3/2}/C_D$ in addition to improving propeller efficiency, reducing specific fuel consumption, carrying more fuel, and flying at lower altitude. Substituting Eq. (34) into Eq. (33) and then into Eq. (77), we have

$$E_{\max} = \frac{1}{\lambda_A^{3/2}} \cdot \frac{1}{4} \frac{\eta_{\text{pr}}}{c} \sqrt{2\rho_a S_{\text{aero}}} \left(\frac{3}{KC_{D0}^{1/3}}\right)^{3/4} (W_1^{-1/2} - W_T^{-1/2}) \tag{78}$$

H. Comparison of Hybrid Airship and Airplane

This subsection is to preliminarily compare the steady flight performance of a hybrid airship and airplane. This comparison is performed on the condition that flight altitude, engine efficiency, fuel consumption are the same.

If the difference of K and C_{D0} can be neglected from the derivation of steady flight performance of a hybrid airship, the following can be concluded:

1) The characteristic velocities of a hybrid airship, such as those for minimum thrust required [Eq. (14)], maximum lift-to-drag ratio [Eq. (27)], minimum power required [Eq. (37)], maximum rate of climb [Eq. (55)], minimum sinking velocity [Eq. (74)], and stall velocity [Eq. (39)] are characterized by

$$U_{\text{hybrid airship}} \propto \sqrt{\frac{\Delta W}{S_{\text{aero}}}}$$

When their effective wing loadings are equal,

$$\frac{U_{\text{hybrid airship}}}{U_{\text{airplane}}} = 1$$

and when their W_T are equal,

$$\frac{U_{\text{hybrid airship}}}{U_{\text{airplane}}} = \sqrt{\lambda_A}$$

2) With the same W_T,

$$\frac{T_{(R)\min,\text{hybrid airship}}}{T_{(R)\min,\text{airplane}}} = \lambda_A$$

3)

$$\frac{(L/D)_{\max,\text{hybrid airship}}}{(L/D)_{\max,\text{airplane}}} = \frac{1}{\lambda_A}$$

4) The minimum power required is characterized by

$$P_{(R)\min,\text{hybrid airship}} \propto \lambda_A W_T, \qquad P_{(R)\min,\text{hybrid airship}} \propto \sqrt{\frac{\Delta W}{S_{\text{aero}}}}$$

With the same effective wing loading and W_T,

$$\frac{P_{(R)\min,\text{hybrid airship}}}{P_{(R)\min,\text{airplane}}} = \lambda_A$$

5) The maximum climb rate is characterized by

$$R/C_{\max,\text{hybrid airship}} \propto -\sqrt{\frac{\Delta W}{S_{\text{aero}}}}, \qquad R/C_{\max,\text{hybrid airship}} \propto \frac{1}{\lambda_A W_T}$$

With the same effective wing loading and W_T,

$$R/C_{\max,\text{hybrid airship}} > R/C_{\max,\text{airplane}}$$

The less λ_A is, i.e., the more buoyancy lift is, and the higher $R/C_{\max,\text{hybrid airship}}$ can be achieved.

6) With the same W_T,

$$\frac{R_{\max,\text{hybrid airship}}}{R_{\max,\text{airplane}}} = \frac{1}{\lambda_A}$$

With the same W_T and S_{aero},

$$\frac{E_{\max,\text{hybrid airship}}}{E_{\max,\text{airplane}}} = \frac{1}{\lambda_A^{3/2}}$$

From Eq. (25), it is clear that the value of λ_A for maximum lift-to-drag ratio is not a constant as reported in [4]. If maximizing L/D is the design object of the hybrid airship, λ_A should be taken as one of the design variables because it greatly affects L/D. Taking the winged hybrid airship as an example, if λ_A increases, the aerodynamic lift will increase and the aerodynamic reference area becomes larger. It makes the wing span efficiency increase so that the induced drag factor K increases. On the other hand, increase of λ_A leads to decrease of airship volume and increase of wing reference area. As change of the airship volume has more effect on C_{D0} than the wing reference area does, C_{D0} decreases due to the smaller airship volume. If the increase value of $\lambda_A\sqrt{K}$ is larger than the decrease value of $\sqrt{C_{D0}}$, then $(L/D)_{\max}$ decreases.

As we all know, wing loading and thrust-to-weight (or power-to-weight) ratio are two key parameters in the conceptual design of an airplane. From the derivations in this section, it can be concluded that the effect of $\Delta W/S_{\text{aero}}$ and $P/\Delta W$ on the steady flight performance of a hybrid airship is identical to that of an airplane. In addition, λ_A also greatly affects the steady flight performance of a hybrid airship.

IV. Analysis of Accelerated Flight Performance

In this section the new formulas for analyzing accelerated flight performance of a hybrid airship are derived. The capacities of level-turn, pull-up, and pull-down maneuvers and taking off and landing will be discussed. Although some accelerated flight characteristics such as minimum turn radius and maximum turning rate are important performances for a fighter aircraft, and hybrid airships are generally not for fighting, these performance characteristics are also discussed for deeper understanding of the flight performance of hybrid airships.

A. Level Turn

The flight path and forces for a hybrid airship in a level turn are sketched in Fig. 3. As shown in Fig. 3, the equations of motion for level turn can be written as

$$L_{\text{aero}}\cos\varphi + L_{\text{buoy}} = W_T \tag{79}$$

$$m_T\frac{U^2}{R_T} = L_{\text{aero}}\sin\varphi \tag{80}$$

The load factor

$$n = L_{\text{aero}}/\Delta W \tag{81}$$

Since Eqs. (79) and (81) hold, we have

$$\varphi = \arccos\frac{1}{n} \tag{82}$$

It can be derived from Eq. (80) that

$$R_T = \frac{m_T U^2}{L_{\text{aero}}\sin\varphi} = \frac{W_T U^2}{gL_{\text{aero}}\sin\varphi} \tag{83}$$

Substituting Eq. (82) into Eq. (83),

$$R_T = \frac{W_T U^2}{gL_{\text{aero}}}\cdot\frac{n}{\sqrt{n^2-1}} \tag{84}$$

Since Eq. (81) and $\lambda_A = \Delta W/W_T$ hold, the final expression for level-turn radius is obtained

$$R_T = \frac{1}{\lambda_A}\cdot\frac{U^2}{g\sqrt{n^2-1}} \tag{85}$$

As the turn rate $\omega_T = U/R_T$, substitute Eq. (85) into it and get

$$\omega_T = \lambda_A\cdot\frac{g\sqrt{n^2-1}}{U} \tag{86}$$

In level-turn flight, the drag is

$$D = \tfrac{1}{2}\rho_a U^2 S_{\text{aero}}(C_{D0} + KC_{L\text{aero}}^2) \tag{87}$$

Substituting Eq. (81) into Eq. (5), we have

$$C_{L\text{aero}} = \frac{n\cdot\Delta W}{\frac{1}{2}\rho_a U^2 S_{\text{aero}}} \tag{88}$$

As $T = D$ and Eq. (88) hold, the expression of n can be solved from Eq. (87):

$$n = \left(\frac{\frac{1}{2}\rho_a U^2}{K(\Delta W/S_{\text{aero}})}\cdot\left(\frac{T}{\Delta W} - \frac{1}{2}\rho_a U^2\frac{C_{D0}}{\Delta W/S_{\text{aero}}}\right)\right)^{1/2} \tag{89}$$

The maximum load factor is constrained by the maximum thrust available:

$$n_{\max} = \left(\frac{\frac{1}{2}\rho_a U^2}{K(\Delta W/S_{\text{aero}})}\cdot\left(\left(\frac{T}{\Delta W}\right)_{\max} - \frac{1}{2}\rho_a U^2\frac{C_{D0}}{\Delta W/S_{\text{aero}}}\right)\right)^{1/2} \tag{90}$$

The conditions for minimum R_T are found by setting $\mathrm{d}R_T/\mathrm{d}U = 0$. Write Eq. (85) in terms of dynamic pressure q for simplifying derivation, which is

$$R_T = \frac{1}{\lambda_A}\cdot\frac{2q}{\rho_a g\sqrt{n^2-1}} \tag{91}$$

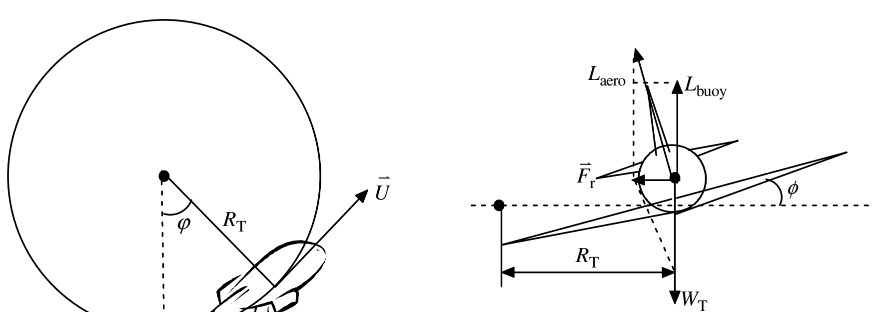

Fig. 3 Hybrid airship in level turn.

Differentiate Eq. (91) with respect to q and set it equal to zero:

$$n^2 - 1 - qn \cdot \frac{\mathrm{d}n}{\mathrm{d}q} = 0 \tag{92}$$

Write Eq. (89) in terms of q, and we have

$$n = \left(\frac{q}{K(\Delta W/S_{\text{aero}})} \left(\frac{T}{\Delta W} - q \cdot \frac{C_{D0}}{\Delta W/S_{\text{aero}}} \right) \right)^{1/2} \tag{93}$$

The following form can also be obtained by differentiation:

$$n \frac{\mathrm{d}n}{\mathrm{d}q} = \frac{T/\Delta W}{2K(\Delta W/S_{\text{aero}})} - \frac{qC_{D0}}{K(\Delta W/S_{\text{aero}})^2} \tag{94}$$

Substituting Eqs. (93) and (94) into Eq. (92) and solving it, the dynamic pressure at which R_T achieves minimum is obtained after simplifications:

$$q_{(R_T)\min} = \frac{2K(\Delta W/S_{\text{aero}})}{T/\Delta W} \tag{95}$$

So

$$U_{(R_T)\min} = \sqrt{\frac{4K(\Delta W/S_{\text{aero}})}{\rho_a(T/\Delta W)}} \tag{96}$$

$$n_{(R_T)\min} = \sqrt{2 - \frac{4KC_{D0}}{(T/\Delta W)^2}} \tag{97}$$

Substituting Eqs. (96) and (97) into Eq. (91), the final expression for minimum R_T is derived:

$$R_{T\min} = \frac{1}{\lambda_A} \cdot \frac{4K(\Delta W/S_{\text{aero}})}{g\rho_a(T/\Delta W)\sqrt{1 - 4KC_{D0}/(T/\Delta W)^2}} \tag{98}$$

The conditions for maximum ω_T are found by setting $\mathrm{d}\omega_T/\mathrm{d}U = 0$. Differentiate Eq. (86) with respect to U and the following equation is obtained:

$$\frac{\mathrm{d}\omega_T}{\mathrm{d}U} = \lambda_A g \cdot \frac{nU \frac{\mathrm{d}n}{\mathrm{d}U} - n^2 + 1}{U^2\sqrt{n^2 - 1}} \tag{99}$$

Differentiating Eq. (89) with respect to U, we get

$$n \frac{\mathrm{d}n}{\mathrm{d}U} = \frac{1}{2} \left(\frac{\rho_a U(T/\Delta W)}{K(\Delta W/S_{\text{aero}})} - \frac{\rho_a^2 U^3 C_{D0}}{K(\Delta W/S_{\text{aero}})^2} \right) \tag{100}$$

Substituting Eqs. (89) and (100) into Eq. (99), the flight velocity at which ω_T achieves the maximum is obtained:

$$U_{(\omega T)\max} = \left(\frac{2(\Delta W/S_{\text{aero}})}{\rho_a} \right)^{1/2} \left(\frac{K}{C_{D0}} \right)^{1/4} \tag{101}$$

The corresponding load factor can be derived by substituting Eq. (101) into Eq. (89), as expressed as

$$n_{(\omega T)\max} = \left(\frac{T/\Delta W}{\sqrt{KC_{D0}}} - 1 \right)^{1/2} \tag{102}$$

Substituting Eqs. (101) and (102) into Eq. (86), the final expression for maximum ω_T is obtained:

$$\omega_{T\max} = \lambda_A g \sqrt{\frac{\rho_a}{\Delta W/S_{\text{aero}}} \left(\frac{T/\Delta W}{2K} - \left(\frac{C_{D0}}{K} \right)^{1/2} \right)} \tag{103}$$

B. Pull-Up and Pull-Down Maneuvers

The flight path and forces for a hybrid airship in pull-up maneuver are shown in Fig. 4.

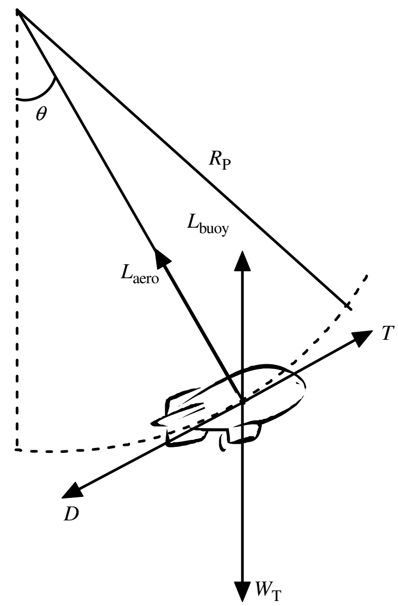

Fig. 4 Pull-up maneuver.

The equation of pull-up motion is given by

$$m_T \frac{U^2}{R_P} = L_{\text{aero}} - \Delta W \cos\theta \tag{104}$$

The instantaneous pull-up is of much greater interest. This corresponds to $\theta = 0$. Then R_P can be derived from Eq. (104):

$$R_P = \frac{W_T/\Delta W}{g} \cdot \frac{U^2}{L_{\text{aero}}/\Delta W - 1} \tag{105}$$

Since Eq. (81) and $\lambda_A = \Delta W/W_T$ hold, Eq. (105) becomes

$$R_P = \frac{1}{\lambda_A} \cdot \frac{U^2}{g(n-1)} \tag{106}$$

As the pull-up rate $\omega_P = U/R_P$,

$$\omega_P = \lambda_A \cdot \frac{g(n-1)}{U} \tag{107}$$

A related case is the pull-down maneuver, as shown in Fig. 5.

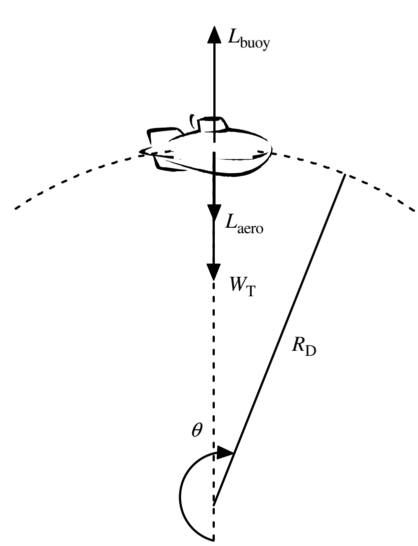

Fig. 5 Pull-down maneuver.

The equation of pull-down motion is given by

$$m_T \frac{U^2}{R_D} = L_{\text{aero}} + \Delta W \tag{108}$$

One can derive the expression for R_D after simplifications:

$$R_D = \frac{W_T/\Delta W}{g} \cdot \frac{U^2}{L_{\text{aero}}/\Delta W + 1} \tag{109}$$

Since Eq. (81) and $\lambda_A = \Delta W/W_T$ hold, Eq. (109) becomes

$$R_D = \frac{1}{\lambda_A} \cdot \frac{U^2}{g(n+1)} \tag{110}$$

As the pull-down rate $\omega_D = U/R_D$,

$$\omega_D = \lambda_A \cdot \frac{g(n+1)}{U} \tag{111}$$

C. Takeoff Performance

In the following two subsections, the takeoff and landing performance of a hybrid airship will be discussed. These discussions are limited to the hybrid airships equipped with conventional turboprops. For some kinds of hybrid airships equipped with vertical takeoff and landing capability, it makes some difference that the ground-roll distances for takeoff and landing are both zero.

The takeoff path of a hybrid airship is sketched in Fig. 6.

1. *Ground Roll* $S_{g,\text{TO}}$

The equation of ground-roll motion is

$$m_T \frac{\mathrm{d}U}{\mathrm{d}t} = T - D - \mu_r(\Delta W - L_{\text{aero}}) \tag{112}$$

where μ_r is the coefficient of rolling friction. Defining S as the rolling distance, we can write

$$\mathrm{d}\,S = \frac{\mathrm{d}U^2}{2\,\mathrm{d}U/\mathrm{d}t} \tag{113}$$

Equation (112) can be written as

$$\frac{\mathrm{d}U}{\mathrm{d}t} = \frac{1}{m_T}(T - D - \mu_r(\Delta W - L_{\text{aero}})) \tag{114}$$

Substituting Eq. (114) into Eq. (113) and integrating it from point 0 to liftoff, we have

$$S_{g,\text{TO}} = \frac{W_T}{2g}\int_0^{U_{\text{LO}}} \frac{\mathrm{d}U^2}{T - D - \mu_r(\Delta W - L_{\text{aero}})} \tag{115}$$

The liftoff velocity is usually set to $U_{\text{LO}} = 1.1U_{\text{stall}}$. As $T - D - \mu_r(\Delta W - L_{\text{aero}})$ does not change greatly in the region from point 0 to liftoff, assume it to be a constant [5]:

$$(T - D - \mu_r(\Delta W - L_{\text{aero}}))_{0.7U_{\text{LO}}}$$

The following expression for $S_{g,\text{TO}}$ can be obtained:

$$S_{g,\text{TO}} = \frac{1}{\lambda_A} \cdot \frac{\Delta W \cdot U_{\text{LO}}^2}{2g} \cdot \frac{1}{(T/\Delta W - D/\Delta W - \mu_r(1 - L_{\text{aero}}/\Delta W))_{0.7U_{\text{LO}}}} + NU_{\text{LO}} \tag{116}$$

where N is the time for ground-roll during rotation. The second term on the right-hand side of Eq. (116) is the distance for the rotation case [5]. Assuming $T \gg D - \mu_r(\Delta W - L_{\text{aero}})$ and substituting U_{LO} into Eq. (116), $S_{g,\text{TO}}$ can be approximated as

$$S_{g,\text{TO}} \approx \frac{1}{\lambda_A} \cdot \frac{1.21(\Delta W/S_{\text{aero}})}{g\rho_a C_{(L\text{aero})\max}(T/\Delta W)_{0.7U_{\text{LO}}}} + 1.1N\sqrt{\frac{2}{\rho_a} \cdot \frac{\Delta W}{S_{\text{aero}}} \cdot \frac{1}{C_{(L\text{aero})\max}}} \tag{117}$$

2. *Distance to Clear an Obstacle* S_c

The distance to clear an obstacle is written as

$$S_c = R_{\text{OB}} \sin\theta_{\text{OB}} \tag{118}$$

It is assumed that the velocity is $1.15U_{\text{stall}}$ and $C_{L\text{aero}}$ is $0.9C_{(L\text{aero})\max}$ [5]. Then $n = 1.19$. Set $H_{\text{OB,TO}}$ as the obstacle height that the hybrid airship clears to take off. From the equation of pull-up radius, Eq. (106), it can be derived that

$$R_{\text{OB}} = \frac{1}{\lambda_A} \cdot \frac{6.96U_{\text{stall}}^2}{g} = \frac{1}{\lambda_A} \cdot \frac{13.92}{\rho_a g} \cdot \frac{\Delta W/S_{\text{aero}}}{C_{(L\text{aero})\max}} \tag{119}$$

$$\theta_{\text{OB}} = \arccos\left(1 - \frac{H_{\text{OB,TO}}}{R_{\text{OB}}}\right) \tag{120}$$

D. Landing Performance

The landing path of a hybrid airship is sketched in Fig. 7.

1. *Approach Distance* S_a

Figure 8 shows the forces applied on hybrid airship on the landing approach flight path. The equations of motion are written as

$$L_{\text{aero}} = W_T\cos\theta_a - L_{\text{buoy}}\cos\theta_a = \Delta W\cos\theta_a \tag{121}$$

$$D = T + W_T\sin\theta_a - L_{\text{buoy}}\sin\theta_a = T + \Delta W\sin\theta_a \tag{122}$$

The approach angle is usually small for most cases. Raymer [8] states that for transport aircraft, $\theta_a \leq 3°$; hence, $\cos\theta_a \approx 1$. Equation (121) becomes

$$L_{\text{aero}} = \Delta W \tag{123}$$

Substituting Eq. (123) into Eq. (122), we have

$$\sin\theta_a = \frac{1}{L_{\text{aero}}/D} - \frac{T}{\Delta W} \tag{124}$$

As $\theta_f = \theta_a$, the flare height

$$H_f = R_f(1 - \cos\theta_a) \tag{125}$$

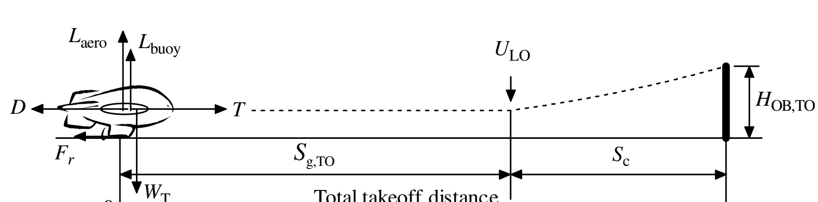

Fig. 6 Illustration of ground roll, airborne distance, and total takeoff distance.

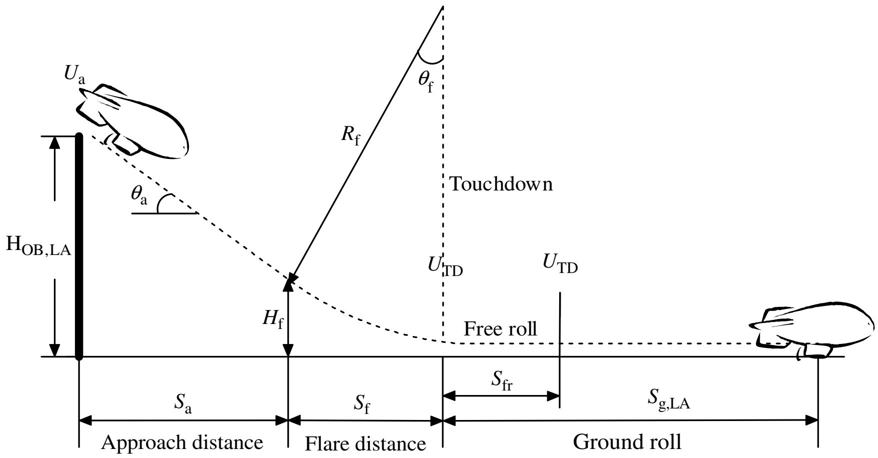

Fig. 7 Landing path and landing distance.

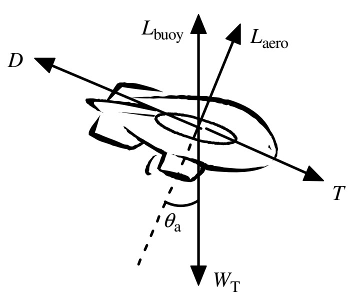

Fig. 8 Force diagram for a hybrid airship on landing approach flight path.

With average flight velocity $U_f = 1.23U_{stall}$ and load factor stipulated as $n = 1.2$, Eq. (106) yields

$$R_f = \frac{1}{\lambda_A} \cdot \frac{U_f^2}{0.2g} = \frac{1}{\lambda_A} \cdot \frac{7.5645U_{stall}^2}{g} = \frac{1}{\lambda_A} \cdot \frac{15.129}{\rho_a g} \cdot \frac{\Delta W/S_{aero}}{C_{(Laero)\max}} \tag{126}$$

The approach distance can be obtained from

$$S_a = \frac{H_{OB,LA} - H_f}{\tan\theta_a} \tag{127}$$

2. Flare Distance S_f

As $\theta_f = \theta_a$, the flare distance is obtained from Fig. 8 as

$$S_f = R_f \sin\theta_a \tag{128}$$

3. Ground Roll $S_{g,LA}$

Figure 9 shows the forces applied on hybrid airship on the landing ground roll. The equation of motion is written as

$$m_T \frac{dU}{dt} = -T_{rev} - D - \mu_r(\Delta W - L_{aero}) \tag{129}$$

where T_{rev} is negative thrust produced by reversible propellers. Solve dU/dt from Eq. (129), substitute it into Eq. (113), and integrate it between the end of the roll (where $U = U_{TD}$) and the complete stop (where $U = 0$), we have

$$S_{g,LA} - S_{fr,LA} = \int_{U_{TD}}^{0} \frac{dU^2}{-T_{rev} - D - \mu_r(\Delta W - L_{aero})} \quad \text{or}$$
$$S_{g,LA} = NU_{TD} + \frac{W_T}{2g}\int_0^{U_{TD}} \frac{dU^2}{T_{rev} + D + \mu_r(\Delta W - L_{aero})} \tag{130}$$

As $T_{rev} + D + \mu_r(\Delta W - L_{aero})$ does not change greatly in the integration region, assume it to be a constant [5]:

$$(T_{rev} + D + \mu_r(\Delta W - L_{aero}))_{0.7U_{TD}}$$

The following expression for $S_{g,LA}$ can be obtained:

$$S_{g,LA} = \frac{1}{\lambda_A}\frac{\Delta W \cdot U_{TD}^2}{2g} \cdot \frac{1}{(T_{rev} + D + \mu_r(\Delta W - L_{aero}))_{0.7U_{TD}}} + NU_{TD} \tag{131}$$

The touchdown velocity is usually set to $U_{TD} = 1.15U_{stall}$; substitute it into Eq. (131), and $S_{g,LA}$ is expressed after reorganization as

$$S_{g,LA} = \frac{1}{\lambda_A} \cdot \frac{1.3225\Delta W/S_{aero}}{g\rho_a C_{(Laero)\max}(T_{rev}/\Delta W + D/\Delta W + \mu_r(1 - L_{aero}/\Delta W))_{0.7U_{TD}}} + 1.15N\sqrt{\frac{2}{\rho_a}\frac{\Delta W}{S_{aero}}\frac{1}{C_{(Laero)\max}}} \tag{132}$$

E. Comparison of Hybrid Airship, Airplane, and Airship

This subsection is to preliminarily compare the accelerated flight performance of a hybrid airship, airplane, and airship. This comparison is performed on the condition that flight altitude, engine efficiency, and fuel consumption are the same.

1) The level-turn, pull-up, and pull-down maneuvers of a hybrid airship are characterized by

$$R_{T\min} \propto 1/\lambda_A, \qquad \omega_{\max} \propto \lambda_A, \qquad R_P \propto 1/\lambda_A$$
$$\omega_P \propto \lambda_A, \qquad R_D \propto 1/\lambda_A, \qquad \omega_D \propto \lambda_A$$

which indicate that the hybrid airship is slower than the airplane ($\lambda_A = 1$) and faster than the airship ($\lambda_A \to 0$) in level-turn, pull-up, and pull-down maneuvers.

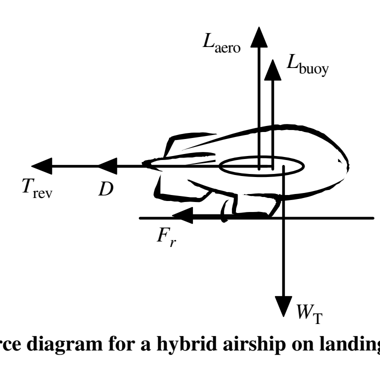

Fig. 9 Force diagram for a hybrid airship on landing ground roll.

Table 1 Comparison of proposed method with existing methods

Flight performance	Airplane [5]	Hybrid airship (this paper)	Hybrid airship [4]
$C_{L\text{buoy}}$	None	$(1-\frac{\rho_h}{\rho_a})\cdot\frac{\rho_{h,c}}{\rho_h}$	$1-\frac{\rho_h}{\rho_a}$
$C_{L\text{aero}}$ ($C_{L\text{wing}}$)	Same	$\frac{L_{\text{aero}}}{\frac{1}{2}\rho_a U^2 S_{\text{aero}}}$	Same
C_L	$C_{L\text{wing}}$	$C_{L\text{buoy}}R_F + C_{L\text{aero}}$	Same
$U_{(TR)\,\min}$	Similar (W_T/S_{wing})	$(\frac{2}{\rho_a}\sqrt{\frac{K}{C_{D0}}}\frac{\Delta W}{S_{\text{aero}}})^{1/2}$	Same
$(T/W)_{\min}$	Similar (T/W_T)	$(T_R/\Delta W)_{\min}=\sqrt{4KC_{D0}}$	Same
$U_{(L/D)\,\max}$	Similar (W_T/S_{wing})	$\sqrt{\frac{2}{\rho_a}\cdot\sqrt{\frac{K}{C_{D0}}}\cdot\frac{\Delta W}{S_{\text{aero}}}}$	$0.891\sqrt{\frac{2}{\rho_a}\cdot\sqrt{\frac{K}{C_{D0}}}\cdot\frac{W_T}{S_{\text{wing}}}}$
$C_{L,(L/D)\,\max}$	Similar ($\lambda_A=1$)	$\frac{1}{\lambda_A}\sqrt{\frac{C_{D0}}{K}}$	Similar ($\lambda_A=0.8$)
$(\frac{L}{D})_{\max}$	Similar ($\lambda_A=1$)	$\frac{1}{\lambda_A}\sqrt{\frac{1}{4KC_{D0}}}$	Similar ($\lambda_A=0.4$)
$U_{(PR)\,\min}$, $U_{(R/C)\,\max}$	Similar (W_T/S_{wing})	$(\frac{2}{\rho_a}\cdot\frac{\Delta W}{S_{\text{aero}}}\sqrt{\frac{K}{3C_{D0}}})^{1/2}$	$(\frac{2}{\rho_a}\cdot\frac{W_T}{S_{\text{wing}}})^{1/2}\times(\frac{1}{\sqrt{3C_{D0}/K+4R_F^2C_{L\text{ship}}^2}-R_FC_{L\text{ship}}})^{1/2}$
$C_{L,(PR)\,\min}$, $C_{L,(UV)\,\min}$	Similar ($\lambda_A=1$)	$\frac{1}{\lambda_A}\sqrt{\frac{3C_{D0}}{K}}$	$\sqrt{3C_{D0}/K+4R_F^2C_{L\text{ship}}^2}-R_FC_{L\text{ship}}$
$(C_L^{3/2}/C_D)_{\max}$	Similar ($\lambda_A=1$)	$\frac{1}{\lambda_A^{3/2}}\cdot\frac{1}{4}(\frac{3}{KC_{D0}^{1/3}})^{3/4}$	None
$P_{(R)\,\min}$	Similar ($\lambda_A=1$, W_T/S_{wing})	$\sqrt{\frac{32\Delta W^2}{\rho_a}\cdot\frac{\Delta W}{S_{\text{aero}}}\cdot(\frac{KC_{D0}^{1/3}}{3})^{3/2}}$	$\sqrt{\frac{2W_t^3}{\rho_a S_{\text{wing}}}\cdot(\frac{C_D^2}{C_L^3})_{\min}}$
U_{stall}	Similar (W_T/S_{wing})	$\sqrt{\frac{2}{\rho_a}\cdot\frac{\Delta W}{S_{\text{aero}}}\cdot\frac{1}{C_{(L\text{aero})\,\max}}}$	$\sqrt{\frac{2}{\rho_a}\cdot\frac{W_T}{S_{\text{wing}}}\cdot\frac{1}{(C_{L\text{ship}}R_F+(C_{L\text{wing}})_{\max})}}$
$U_{(\theta)\,\max}$	Similar (W_T/S_{wing}, P/W_T)	$\frac{4(\Delta W/S_{\text{aero}})K}{\rho_a\eta_{\text{pr}}(P_{\text{es}}/\Delta W)}$	$\frac{4K}{\rho_a\eta_{\text{pr}}(P/S_{\text{wing}})}\cdot(\frac{\Delta W}{S_{\text{wing}}})^2$
$\theta_{\max}$	None	$\arcsin(f-\frac{KC_{D0}}{f})$, $f=\frac{\rho_a\eta_{\text{pr}}^2(P_{\text{es}}/\Delta W)^2}{8K(\Delta W/S_{\text{aero}})}$	None
$(R/C)_{\max}$	$\cos\theta\approx 1$: similar ($\lambda_A=1$, W_T/S_{wing}), $\cos\theta<1$: None	$\cos\theta\approx 1$: $\frac{1}{\lambda_A}(\frac{\eta_{\text{pr}}P_{\text{es}}}{W_T}-(\frac{2}{\rho_a}\sqrt{\frac{K}{3C_{D0}}}\cdot\frac{\Delta W}{S_{\text{aero}}})^{1/2}\cdot\frac{1.155}{(L/D)_{\max}})$, $\cos\theta<1$: $\frac{1}{2\sqrt{3}}(\frac{U_{(R/C)\,\max}}{A}-\sqrt{(\frac{U_{(R/C)\,\max}}{A})^2-4\sqrt{3}B\cdot\frac{U_{(R/C)\,\max}}{A}+16U_{(R/C)\,\max}^2})$, $A=\sqrt{KC_{D0}}$, $B=\frac{\eta_{\text{pr}}P_{\text{es}}}{\Delta W}$	$U((\frac{T}{S_{\text{wing}}}-\frac{1}{2}\rho_aU^2C_{d0})(\frac{\Delta W}{S_{\text{wing}}})^{-1}-\frac{2K(\cos\theta)^2}{\rho_aU^2}\cdot\frac{\Delta W}{S_{\text{wing}}})$
$U_{(V)\,\min}$	Similar (W_T/S_{wing})	$\sqrt{\frac{32}{\rho_a}\cdot\frac{\Delta W}{S_{\text{aero}}}\cdot(\frac{kC_{D0}^{1/3}}{3})^{3/2}}$	$U_V=\sqrt{\frac{2}{\rho_aC_{L\text{wing}}^3/C_D^2}\cdot\frac{\Delta W}{S_{\text{wing}}}}$
$R_{\max}$	Similar ($\lambda_A=1$)	$\frac{1}{\lambda_A}\cdot\frac{\eta_{\text{pr}}}{c}\sqrt{\frac{1}{4KC_{D0}}}\ln\frac{W_T}{W_1}$	$R=\frac{\eta_{\text{pr}}}{c}\frac{L}{D}\ln\frac{W_T}{W_1}$
$E_{\max}$	Similar ($\lambda_A=1$)	$\frac{1}{\lambda_A^{3/2}}\cdot\frac{1}{4}\frac{\eta_{\text{pr}}}{c}\sqrt{2\rho_aS_{\text{aero}}}(\frac{3}{KC_{D0}^{1/3}})^{3/4}(W_1^{-1/2}-W_T^{-1/2})$	$E=\frac{\eta_{\text{pr}}}{c}\sqrt{2\rho_aS_{\text{aero}}}\frac{C_L^{3/2}}{C_D}\cdot(W_1^{-1/2}-W_T^{-1/2})$
$U_{(R_T)\,\min}$	Similar (W_T/S_{wing},T/W_T)	$\sqrt{\frac{4K(\Delta W/S_{\text{aero}})}{\rho_a(T/\Delta W)}}$	Same
$n_{(R_T)\,\min}$	Similar (T/W_T)	$\sqrt{2-\frac{4KC_{D0}}{(T/\Delta W)^2}}$	Same
$R_{T\,\min}$	Similar ($\lambda_A=1$, W_T/S_{wing}, T/W_T)	$\frac{1}{\lambda_A}\cdot\frac{4K(\Delta W/S_{\text{aero}})}{g\rho_a(T/\Delta W)\sqrt{1-4KC_{D0}/(T/\Delta W)^2}}$	$\frac{4K(\Delta W/S_{\text{wing}})}{g\rho_a(T/W_T)\sqrt{1-4KC_{D0}/(T/\Delta W)^2}}$
$U_{(\omega T)\,\max}$	Similar (W_T/S_{wing})	$(\frac{2(\Delta W/S_{\text{aero}})}{\rho_a})^{1/2}(\frac{K}{C_{D0}})^{1/4}$	None
$n_{(\omega T)\,\max}$	Similar (T/W_T)	$(\frac{T/\Delta W}{\sqrt{KC_{D0}}}-1)^{1/2}$	None
$\omega_{T\,\max}$	Similar ($\lambda_A=1$, W_T/S_{wing}, T/W_T)	$\lambda_Ag\sqrt{\frac{\rho_a}{\Delta W/S_{\text{aero}}}(\frac{T/\Delta W}{2K}-(\frac{C_{D0}}{K})^{1/2})}$	None
R_P	Similar ($\lambda_A=1$)	$\frac{1}{\lambda_A}\cdot\frac{U^2}{g(n-1)}$	Same
ω_P	Similar ($\lambda_A=1$)	$\lambda_A\cdot\frac{g(n-1)}{U}$	Same
R_D	Similar ($\lambda_A=1$)	$\frac{1}{\lambda_A}\cdot\frac{U^2}{g(n+1)}$	None
ω_D	Similar ($\lambda_A=1$)	$\lambda_A\cdot\frac{g(n+1)}{U}$	None
$S_{g,\text{TO}}$	Similar ($\lambda_A=1$, W_T/S_{wing}, T/W_T)	$\frac{1}{\lambda_A}\cdot\frac{1.21(\Delta W/S_{\text{aero}})}{g\rho_aC_{(L\text{aero})\,\max}(T/\Delta W)_{0.7U_{\text{LO}}}}+1.1N\sqrt{\frac{2}{\rho_a}\cdot\frac{\Delta W}{S_{\text{aero}}}\cdot\frac{1}{C_{(L\text{aero})\,\max}}}$	$\frac{1.21(W_T/S_{\text{wing}})}{g\rho_a(C_{L\text{ship}}R_F+C_{(L\text{wing})\,\max})(T/W_T)_{0.7U_{\text{LO}}}}$
S_c	Similar ($\lambda_A=1$, W_T/S_{wing})	$R_{\text{OB}}\sin\theta_{\text{OB}}$, $R_{\text{OB}}=\frac{1}{\lambda_A}\cdot\frac{6.96U_{\text{stall}}^2}{g}$, $\theta_{\text{OB}}=\arccos(1-\frac{H_{\text{OB,TO}}}{R_{\text{OB}}})$	None

(continued)

Table 1 Comparison of proposed method with existing methods (Continued)

Flight performance	Airplane [5]	Hybrid airship (this paper)	Hybrid airship [4]
$S_{g,\mathrm{LA}}$	Similar ($\lambda_A = 1$, W_T/S_{wing}, T/W_T)	$1.15N\sqrt{\frac{2}{\rho_a}\frac{\Delta W}{S_{\mathrm{aero}}}\frac{1}{C_{(L\mathrm{aero})\max}}} + \frac{1}{\lambda_A}\cdot\frac{1}{g\rho_a C_{(L\mathrm{aero})\max}}$ $\frac{1.3225\Delta W/S_{\mathrm{aero}}}{(T_{\mathrm{rev}}/\Delta W + D/\Delta W + \mu_r(1 - L_{\mathrm{aero}}/\Delta W))_{0.7U_{TD}}}$	$\frac{1}{g\rho_a(C_{L\mathrm{ship}}R_F + C_{(L\mathrm{wing})\max})}$ $\frac{1.21W_T/S_{\mathrm{wing}}}{(D/W_T + \mu_r(1 - L/W_T))}$
S_a	Similar ($\lambda_A = 1$, W_T/S_{wing}, T/W_T)	$\frac{H_{\mathrm{OB,LA}} - R_f(1-\cos\theta_a)}{\tan\theta_a}$, $R_f = \frac{1}{\lambda_A}\cdot\frac{7.5645U^2_{\mathrm{stall}}}{g}$, $\theta_a = \arcsin(\frac{1}{L_{\mathrm{aero}}/D} - \frac{T}{\Delta W})$	None
S_f	Same	$R_f \sin\theta_a$	None

2) When the hybrid airship takes off,

$$S_{g,\mathrm{TO}} \propto \frac{1}{\lambda_A}, \qquad S_{g,\mathrm{TO}} \propto \frac{\Delta W}{S_{\mathrm{wing}}}, \qquad S_{g,\mathrm{TO}} \propto \frac{1}{T/\Delta W}$$

$$R_{\mathrm{OB}} \propto \frac{1}{\lambda_A}, \qquad R_{\mathrm{OB}} \propto \frac{\Delta W}{S_{\mathrm{wing}}}$$

With the same $C_{(L\mathrm{wing})\max}$, effective wing loading, and effective thrust-to-weight ratio,

$$S_{g\mathrm{TO,hybrid\ airship}} > S_{g\mathrm{TO,airplane}}, \qquad R_{\mathrm{OB,hybrid\ airship}} > R_{\mathrm{OB,airplane}}$$

As $\Delta W = \lambda_A W_T$, Eqs. (117) and (119) can be rewritten as

$$S_{g,\mathrm{TO}} \approx \lambda_A \cdot \frac{1.21(W_T/S_{\mathrm{aero}})}{g\rho_a C_{(L\mathrm{aero})\max}(T/W_T)_{0.7U_{\mathrm{LO}}}} + \sqrt{\lambda_A} \cdot 1.1N\sqrt{\frac{2}{\rho_a}\cdot\frac{W_T}{S_{\mathrm{aero}}}\cdot\frac{1}{C_{(L\mathrm{aero})\max}}}$$

$$R_{\mathrm{OB}} = \frac{13.92}{\rho_a g}\cdot\frac{W_T/S_{\mathrm{aero}}}{C_{(L\mathrm{aero})\max}}$$

So with the same $C_{(L\mathrm{aero})\max}$, W_T/S_{aero} and (T/W_T),

$$S_{g\mathrm{TO,hybrid\ airship}} < S_{g\mathrm{TO,airplane}}, \qquad R_{\mathrm{OB,hybrid\ airship}} = R_{\mathrm{OB,airplane}}$$

3) When the hybrid airship lands,

$$R_f \propto \frac{1}{\lambda_A}, \qquad R_f \propto \frac{\Delta W}{S_{\mathrm{aero}}}, \qquad S_{g,\mathrm{LA}} \propto \frac{1}{\lambda_A}$$

$$S_{g,\mathrm{LA}} \propto \frac{\Delta W}{S_{\mathrm{aero}}}, \qquad S_{g,\mathrm{LA}} \propto \frac{1}{T/\Delta W}$$

The landing performance is similar to the takeoff performance for the hybrid airship. So the result of comparison is the same.

V. Comparison with Existing Methods

In this section the analysis method of flight performance proposed in this work will be compared with the existing methods for a hybrid airship [4] and for an airplane [5]. The analysis methods of the main flight performance characteristics are listed in Table 1. In the table, none indicates that it does not exist or it is not provided; same indicates that the formula is the same as that presented in this paper; and similar (exception case) indicates that the formula is similar to that presented in this paper, except that $\lambda_A = 1$, or $\Delta W/S_{\mathrm{aero}}$ is replaced by W_T/S_{wing} or $T/\Delta W$ $(P/\Delta W)$ is replaced by T/W_T (P/W_T), with the exception cases in the parentheses.

As $\Delta W = \lambda_A W_T$, then $\Delta W = W_T$ when $\lambda_A = 1$. It is shown in Table 1 that when $\lambda_A = 1$, the analysis method of flight performance for a hybrid airship can be directly reduced to that of airplane.

Compared with the method in [4], this work mainly contributes to the following:

1) The new formulas for analyzing steady and accelerated flight of a hybrid airship are systematically derived to the simplest expression. All of these formulas are written in the expression of three key design parameters: λ_A, $\Delta W/S_{\mathrm{aero}}$, and $T/\Delta W$ (or $P/\Delta W$). It can be concluded from Table 1 that most formulas in [4] [such as $P_{(R)\min}$, U_{stall}, $(R/C)_{\max}$, and $U_{(V)\min}$] have not been derived to the simplest expression and the corresponding flight performances have to be analyzed by iteration.

2) The expression for maximum lift-to-drag ratio is corrected. According to the optimization principle, the objective function can be maximized or minimized by differentiating it with respect to all the independent design variables and setting the results equal to zero. In [4], Eq. (17) was differentiated with respect to C_L and $R_F C_{L\mathrm{buoy}}$, respectively, for maximizing L/D. However, C_L and $R_F C_{L\mathrm{buoy}}$ are actually not independent of each other according to Eq. (6). In this paper R_F is derived as the function of C_L in Eq. (19) and substituted into Eq. (17). Then the revised form of the maximum L/D and

Table 2 Design parameters of the model hybrid airship

Parameters	Values
Total weight, N	19
Airship body	
Volume, m^3	1.08
Gross buoyant lift, N	13.3
Front-projected area, m^2	0.98
Maximum length, m	2.3
Maximum diameter, m	1.1
Horizonal fin area, m^2	0.25
Vertical fin area, m^2	0.126
Wing	
Wing section	NACA4312
Area, m^2	0.309
Span, m	1.52
Chord, m	0.203
Vertical tail	
Cross section	Flat plate
Area, m^2	0.053
Rudder area	0.053
Horizontal tail	
Cross section	Flat plate
Area, m^2	0.155
Elevator area, m^2	0.155

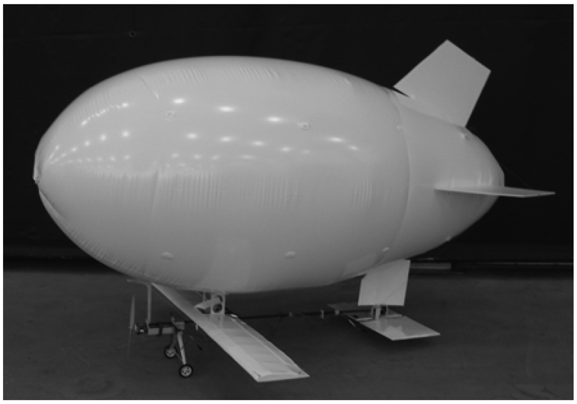

Fig. 10 Remote-controllable model aeroship [9].

Table 3 Estimated and measured flight performance parameters for a model hybrid airship

Parameter	Estimated	Measured in flight
Maximum R/C, m/s	2.4	2.5
Angle at maximum R/C, deg	40.6	32.3
Velocity at maximum R/C, m/s	3.7	4.5
Stall velocity, m/s	5.3	4.2
Minimum level-turn radius, m	3.4	3.6
Takeoff ground roll, m	6.2	3
Takeoff velocity, m/s	5.8	4.2
Approach angle in landing, deg	13.9	16.7
Touchdown velocity in landing, m/s	6.2	3.3

Table 4 Other estimated flight performance parameters

Parameter	Estimated
Minimum required thrust, N	1.3
Velocity at maximum L/D, m/s	4.9
Maximum L/D	14.2
Minimum required power, W	5.8
Minimum sinking velocity, m/s	0.8
Minimum glide angle, deg	10
Velocity at minimum turn radius, m/s	3.4
Load factor at minimum turn radius	1.3
Maximum turn rate, s^{-1}	1.2
Velocity at maximum turn rate, m/s	4.9
Load factor at maximum turn rate	1.8
Landing ground roll, m	9.5

its corresponding velocity and lift coefficient are obtained. Equation (19) is also substituted into Eq. (31). Then the revised form of the minimum P_R and its corresponding velocity and lift coefficient are obtained.

3) A more general form of buoyant lift coefficient is proposed. For nonrigid and semirigid airships, volume changes of the lifting gas, due to temperature changes, are balanced using a ballonet in order to maintain the overpressure and then maintain the shape of the airship body. This case is considered in the derivation of buoyant lift coefficient in this paper.

VI. Example

To validate the proposed analysis method, the flight performance of a remote-controllable model hybrid airship [9] is estimated and compared with the data measured in flight. Flight testing of the hybrid airship was conducted in [9]. Figure 10 shows the model hybrid airship that is a direct combination of a model airplane and a model airship. Table 2 lists the design parameters of the model hybrid airship.

The comparison results are listed in Table 3. The other estimated flight performance parameters are listed in Table 4. From the comparison, the following can be concluded:

1) In general, the computed results are in reasonably good agreement with the data obtained from flight testing. The deviation is due to assumption and simplification in the numerical method as well as error in flight testing.

2) Because of overestimated stall velocity, the takeoff velocity, takeoff ground roll, and touchdown velocity in landing are overestimated and the approach angle in landing is underestimated.

3) Because of underestimated velocity at maximum R/C, the angle at maximum R/C is overestimated.

VII. Conclusions

Taking the analysis method of flight performance for propeller-driven airplane as a reference, a revised formulation for flight performance analysis of a hybrid airship is systematically derived in this paper, which might be helpful for analyzing flight performance of hybrid airships, for better understanding of the mechanism of hybrid airships and for the design of hybrid airships. Compared with the existing method of flight performance for hybrid airships, each proposed formula is expressed in the simplest form as a function of λ_A, $\Delta W/S_{\text{aero}}$, and $T/\Delta W$ ($P/\Delta W$), which can be directly reduced to the corresponding formula for an airplane by setting $\lambda_A = 1$. Furthermore, some errors in the existing method of hybrid airships are corrected. The relationship between flight performances of a hybrid airship and airplane are clearly indicated in these new formulas. The theoretical comparisons based on these formulas are made to identify the positive and negative aspects of hybrid airships. An example of estimating flight performance of a model hybrid airship is presented to preliminarily demonstrate and evaluate the developed method, which shows a reasonable result.

Acknowledgments

This research has benefited greatly from the support of NSFC (National Natural Science Foundation of China) under grant no. 10702055 and Ph.D. Programs Foundation of the Ministry of Education of China under grant no. 20070699047. We would like to acknowledge Tianshu Liu for providing data of the model hybrid airship.

References

[1] Ashford, R. L., Levitt, B. B., Mayer, N. J., Vocar, J. M., and Woodward, D. E., "1981 LTA Technology Assessment: Past and Present," AIAA Paper 1981-2348, 1981.

[2] Ardema, M. D., "Feasibility of Modern Airships: Preliminary Assessment," *Journal of Aircraft*, Vol. 14, No. 11, 1977, pp. 1140–1148.
doi:10.2514/3.58902

[3] Boyd, R. R., "Performance of Hybrid Air Vehicles," AIAA Paper 2001-0388, 2001.

[4] Liu, T. S., and Liou, W. W., "Aeroship: A New Flight Platform," AIAA Paper 2006-3922, 2006.

[5] Anderson, J. D., *Aircraft Performance and Design*, McGraw–Hill, Boston, 1999.

[6] Khoury, G. A., and Gillett, J. D., *Airship Technology*, Cambridge Univ. Press, New York, 1999.

[7] Francis, J. H., *Introduction to Aircraft Performance, Selection and Design*, Wiley, New York, 1984.

[8] Raymer, D. P., *Aircraft Design: A Conceptual Approach*, 3rd ed., AIAA, Washington, D.C., 1999.

[9] Liu, T. S., Liou, W. W., and Schulte, M., "Aeroship: A Hybrid Flight Platform," *Journal of Aircraft*, Vol. 46, No. 2, 2009, pp. 667–674.
doi:10.2514/1.39950